ROYAL SOCIETY
OF CHEMISTRY

Check for updates

Morphological and mechanical properties of biodegradable poly(glycolic acid)/poly(butylene adipate-*co*-terephthalate) blends with *in situ* compatibilization†

Rong Wang, [iD] * Xiaojie Sun, Lanlan Chen and Wenbin Liang

In the present work, the biodegradable blends of poly(glycolic acid) (PGA) and poly(butylene adipate-*co*-terephthalate) (PBAT) with *in situ* compatibilization using 4,4′-methylenebis(phenyl isocyanate) (MDI) were prepared. The combined results of FTIR, DSC, SEM, DSC, POM, TGA and rheology demonstrated that the MDI was successfully reacted with PGA/PBAT, the complex viscosity and storage moduli (G') of the blends were increased. Melt elasticity and viscosity of the blends were also increased on increasing the concentration of PBAT. SEM results indicated that the compatibility was improved by *in situ* compatibilization. Due to the apparent differences in melting temperature (T_m) between PGA and PBAT, the morphology of the dispersed phase evolved from a spherical structure to *in situ* microfiber when the content of PBAT was up to 60% during injection molding. The interfacial adhesion between PGA and PBAT was strengthened, consequently, the impact strength of the blend was sharply increased from 9.0 kJ m^{-2} to 22.2 kJ m^{-2}. On account of the chain extension effect, the crystallinity, crystallization temperature and crystallization size were decreased, which was also of benefit for the improvement of toughness. Meanwhile, the thermal stability of the PGA was improved through blending with PBAT. A novel biodegradable blending material with enhanced toughness and thermal stability was prepared.

1. Introduction

With the tremendous attention to environmental protection, biodegradable polymers arouse great interest for both industry and academia. To solve the "white pollution" caused by petroleum-based materials, the current trend is employing biodegradable materials as a promising replacement. However, the limited production and poor mechanical properties of most biopolymers have severely hindered their applications. Therefore, the development of novel biopolymer systems with high performance is of vital importance.[1,2]

Polyglycolic acid (PGA) is a kind of biopolymer with the simplest aliphatic ester structure. The biodegradability and biocompatibility of PGA are excellent, while the polymerization of high molecular weight PGA is extremely difficult. As a result, the price is quite high, and the application of PGA is basically realized in medical field at present.[3,4] However, due to its crystallizable ability and high density, PGA possesses many other outstanding properties, especially gas barrier and mechanical properties.[5] The gas barrier ability of PGA is 100 times of PET

and 1000 times of PLA, meanwhile its mechanical strength (flexural modulus: ∼7.0 GPa, tensile strength: ∼110 MPa) equals or exceeds that of other resins. On the other hand, with the development of PGA polymerization technology, quantitative production is imminent.[6] Therefore, the applications of PGA can be expanded to the fields of high barrier material, biodegradable packing and so on.[7–10] While, similar to PLA, PGA still has some defects such as poor toughness and thermal stability, which restrict its applications to a great extent. Hence, the toughness modification of PGA is crucial.

One of the common toughening methods was blending with other flexible polymers or plasticizers.[11–13] Various polymers were used in toughening PLA, such as elastomers, glycidyl ester compatibilizers and their copolymers/elastomers, petroleum-based traditional plastics (PE, PP) and various biodegradable polymers.[14,15] To prepare high-performance PLA-based blends, the compatibilizers including non-reactive compatibilizers, reactive polymer compatibilizers or active small molecular substances, and *in situ* formed block copolymers or graft copolymers were used to improve the interfacial compatibility.[16–19] Due to the fully biodegradability, high flexibility,[20] melt strength[21] and heat resistance, poly(butylene adipate-*co*-terephthalate) (PBAT) arouse great interest in toughening PLA.[22–25] L. Jiang *et al.* studied the biodegradable PLA/PBAT blends, the impact strength was increased from 2.7 to 4.5 kJ

National Institute of Clean and Low-Carbon Energy, Beijing, 102211, China. E-mail: rong.wang.cv@chnenergy.com.cn

† Electronic supplementary information (ESI) available. See DOI: 10.1039/d0ra08813g

m^{-2} with the addition of 20 wt% PBAT.[26] To improve the compatibility and optimize the mechanical properties of polymer blends, different compatibilizers and *in situ* reactions were studied. P. Ma *et al.* reported an *in situ* compatibilization of PLA/PBAT blends by using dicumyl peroxide as a free-radical initiator, the compatibility was significantly improved, the elongation at break and the notched izod impact toughness were largely increased.[27] N. W. Zhang *et al.* prepared the PLA/PBAT blends with glycidyl methacrylates (GMA) as reactive agent, it was found that better miscibility and more shear yielding mechanism were responsible for the improved toughness of the blends.[28] MDI, which contains two isocyanate groups, is highly reactive to carboxyl and hydroxyl groups, so it is widely used in the two component systems as a chain extender.[29–31] H. W. Pan *et al.* introduced the MDI to PLA/PBAT blends, due to the chain extension reaction, the PBAT phase size was deduced and the interfacial adhesion was obviously increased.[32] Although the toughening modifications of PLA were widely studied, the research on the PGA was rarely reported.

To develop new biopolymer systems, in this work, the biodegradable PGA/PBAT blends were prepared through melt processing. Meanwhile, MDI was used as chain extender to enhance the compatibility. The effect of the contents of MDI and PBAT on the mechanical properties, morphologies, rheological properties, thermal stabilities and crystallization behaviors were systematically investigated.

2. Experiment

2.1 Materials

All the materials used for this work were commercially available and used as received without further treatments. PGA (M_n = 179 000 g mol^{-1}, Shanghai Pujing Corp.;) PBAT (M_w = 145 000 g mol^{-1}, BASF Corp.); 4,4′-methylenebis(phenyl isocyanate) (MDI, 98%, Innochem).

2.2 Samples preparation

PGA and PBAT were dried at 80 °C in a vacuum oven for 8 h before use. The blends were melt-blended using a Haake twin-screw extruder (Mess-Technic GmbH, Germany) running at 100 rpm at 230 °C. The length–diameter ratio of screw was 21/1. The test specimens were prepared from the extruded blends by using a micro injection molding machine (Haake) with a barrel at 245 °C. The temperature of the mold was 50 °C and the cycle time was approximately 15 s. The injection pressure was 900 bar.

2.3 Measurement

2.3.1 Impact strength. Notched impact strength tests were conducted by using a ZBC14002 impact tester (Sans Group Company) and pendulums of 1 J and 1.5 J were adapted to the standard ISO 179-2003. The notched specimens for test were 80 × 10 × 4 mm^3. Five replicates were tested for each sample to get an average value.

2.3.2 Scanning electron microscope (SEM). The surfaces of fracture-frozen cross sections of the impact test specimens of

PGA/PBAT blends were etched with dichloromethane at room temperature to remove the PBAT. And the samples before and after etch, taken in a transverse way, were coated with gold and observed by SEM (Nova Nano SEM 450).

2.3.3 Differential scanning calorimetry (DSC). Crystallization behaviors of the blends were investigated by a TA Q2000 DSC instrument. Firstly, the samples were heated with a rate of 20 K min^{-1} from room temperature to 230 °C, then it was cooled down to −50 °C with a rate of 2 K min^{-1} under nitrogen. Subsequently, a second heating scan to 230 °C was conducted at the same heating rate. The degree of crystallinity of the samples was evaluated by the following relationship:

The melting enthalpy ΔH_m and T_m were determined at the second heating cycle by removing the heating history.

$$X_c(100\%) = \frac{\Delta H_m}{W_f \Delta H_{fusion}} \times 100\%,$$

where X_c is the degree of crystallinity of the PGA or PBAT, "ΔH_m" is the melting enthalpy determined at the second heating cycle, "W_f" is the weight fraction of PGA or PBAT in the blends and "ΔH_{fusion}" is the enthalpy of fusion for a crystal having infinite crystal thickness (183.2 J g^{-1} for PGA and 114 J g^{-1} for PBAT).[5,32]

2.3.4 Rheological behavior. Rheological behaviors of PGA/PBAT blends were investigated using a strain-controlled rheometer (ARES). Samples were tested using a parallel-plate geometry (d = 25 mm) operated at 240 °C. The blends were tested by dynamic strain sweep test (Fig. S1†) firstly, then the dynamic frequency sweep tests (0.05–100 rad s^{-1}), were done in the range of liner viscoelasticity (2% strain).

2.3.5 Thermal gravimetric analysis (TGA). The thermal stabilities of the samples were evaluated by a TA Q100 TGA instrument. The samples were heated to 600 °C with a rate of 20 K min^{-1} under air, and the 5% decomposition temperatures were obtained.

2.3.6 Polarizing optical microscope (POM). The crystalline structures were observed by Carl Zeiss imager Z1M POM (Germany). Ultrathin sections, prepared from the centers of the injection samples, were used to be observed, and the images were taken at room temperature without heating.

2.3.7 Fourier transform infrared (FTIR). Chemical structures of PGA, PBAT, MDI and the blend (GB3M0.5) were examined using a Fourier transform infrared spectroscopy (Shimadzu, Prestige-21) over the wavenumbers ranging from 4000 to 400 cm^{-1}. The samples PGA, PBAT and the blend (GB3M0.5) were compression-molded into thin film and measured using transmission mode. The MDI were measured as powder using ATR mode.

3. Results and discussions

Unlike PLA, which had been extensively studied for toughening modification, PGA was rarely studied. To get deep insight into the effects of PBAT and MDI, a series of blends with 10, 30, 50, 60, 70 and 80% of PBAT were prepared. And in the corresponding blends, the contents of MDI were also variable. For simplify, the samples were named to GB*x*M*y* (G: abbreviation of PGA; B: abbreviation of PBAT; *x*: the contents of PBAT, the total

contents of PGA and PBAT is 10; M: abbreviation of MDI; y: the contents of MDI). The mechanical properties, morphologies, rheological properties, DSC, POM and thermal stabilities of the blends were investigated.

3.1 Fourier transform infrared (FTIR) spectroscopy analysis

The chain extension reaction of PGA, PBAT with MDI is shown in Scheme 1. As the high reactivity of di-isocyanate towards hydroxyl end group of PGA and PBAT molecules through urethane bonds, complex product mixtures were obtained, including branched PGA, branched PBAT and PGA-crosslink-PBAT structures.[32] The chemical structure of the blend was verified by FTIR spectra as shown in Fig. 1. The stretching band at 2300 cm^{-1}, which corresponded to the isocyanate group of MDI, was not found in the spectra of the resulting blend. Meanwhile, the –N–H absorption peak appeared at 3400 cm^{-1}, indicating that MDI was completely reacted with PGA and PBAT.

3.2 Rheological properties

Due to the chain extension reaction, the molecular weight and the entanglement of chain were enhanced, which might cause the changes in the melt properties. In order to verify this, the rheological properties of the blends were measured. Frequency dependences of storage modulus and loss modulus of PGA/PBAT blends with different contents of MDI and PBAT were listed in Fig. 2. The change trend of energy storage modulus and loss modulus was consistent. Clearly, the addition of MDI led to much higher storage modulus and loss modulus at nearly all frequencies for the PGA/PBAT (40/60) blends as shown in Fig. 2(a). This result indicated that PGA/PBAT blends were effectively reacted with MDI, which introduced more entanglement structures in PGA/PBAT melts. By increasing the contents of MDI, more molecular chains were involved in the reaction, and the storage modulus was further increased. To obtain sufficient compatibility, the content of MDI in other blends with different PBAT contents was fixed at 5%. As shown in Fig. 2(b), with increasing the contents of PBAT, the storage modulus was gradually increased. This was due to the more flexible molecular chain of PBAT than that of PGA, and the former was much easier to entangle. But when the content of PBAT was above 60%, the storage modulus kept steady. Fig. 3 shown the curves
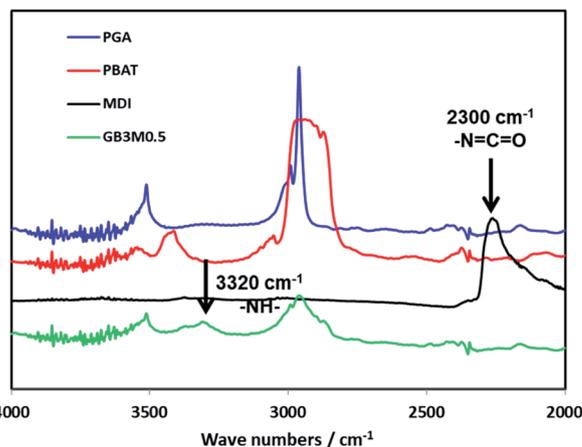

Fig. 1   FTIR spectra of PGA, PBAT, MDI and GB3M0.5.

of the dynamic complex viscosity η^* of PGA/PBAT blends with different contents of MDI and PBAT. Similar to the change rules of storage modulus, through reacting with MDI, the complex viscosity η^* was also greatly enhanced at nearly all frequencies. This phenomenon indicated that the molecular weight of the blends was greatly increased, which resulting in the remarkably hindered movement of molecular chains.[28] The more entanglements of PBAT rendered the increase of complex viscosity of the blends with increasing the contents of PBAT.

3.3 Mechanical properties

The impact strength of the blends was shown in Fig. 4. It can be seen from Fig. 4(a) that when the content of PBAT was less than 70%, the effect of MDI was obvious. The addition of MDI could effectively improve the notched impact strength of the system. However, after the content of PBAT reached 70%, the impact of compatibilizer was suppressed. Furtherly, there was almost no effect when the content of PBAT reached 80%, both of the systems (with or without MDI) had high impact strength. Meanwhile, the content of compatibilizer was fixed in order to research the effect of the content of PBAT on the notched impact. It was found that when the content of PBAT was less than 60%, the effect of the PBAT content on the notched impact was not obvious. But when its content reached 60%, the notched impact increased significantly from 9.0 kJ m^{-2} to 22.2 kJ m^{-2}. The impact strength reached the maximum (56.6 kJ m^{-2}) when the content of PBAT was 70%, and it was reduced along with the further increase of PBAT content.

The elongation at break of the blends was shown in Fig. 5. Consistent with the results of impact strength, the addition of MDI was benefit for improving the elongation when the contents of PBAT was less than 70%, while the effect was disappeared when contents of PBAT reached 80%. Different from the effects of PBAT on the impact strength, the elongation of the systems was obviously increased from 20% to ~100% when 30% PBAT was added, then kept relatively stable up to 70% PBAT, finally increased sharply to ~300% when the content of
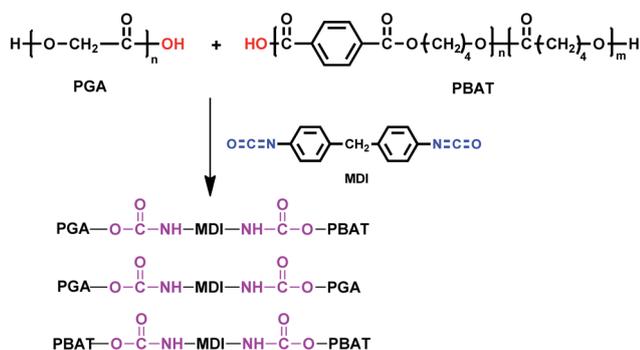
Scheme 1   The reaction of PGA and PBAT with MDI.

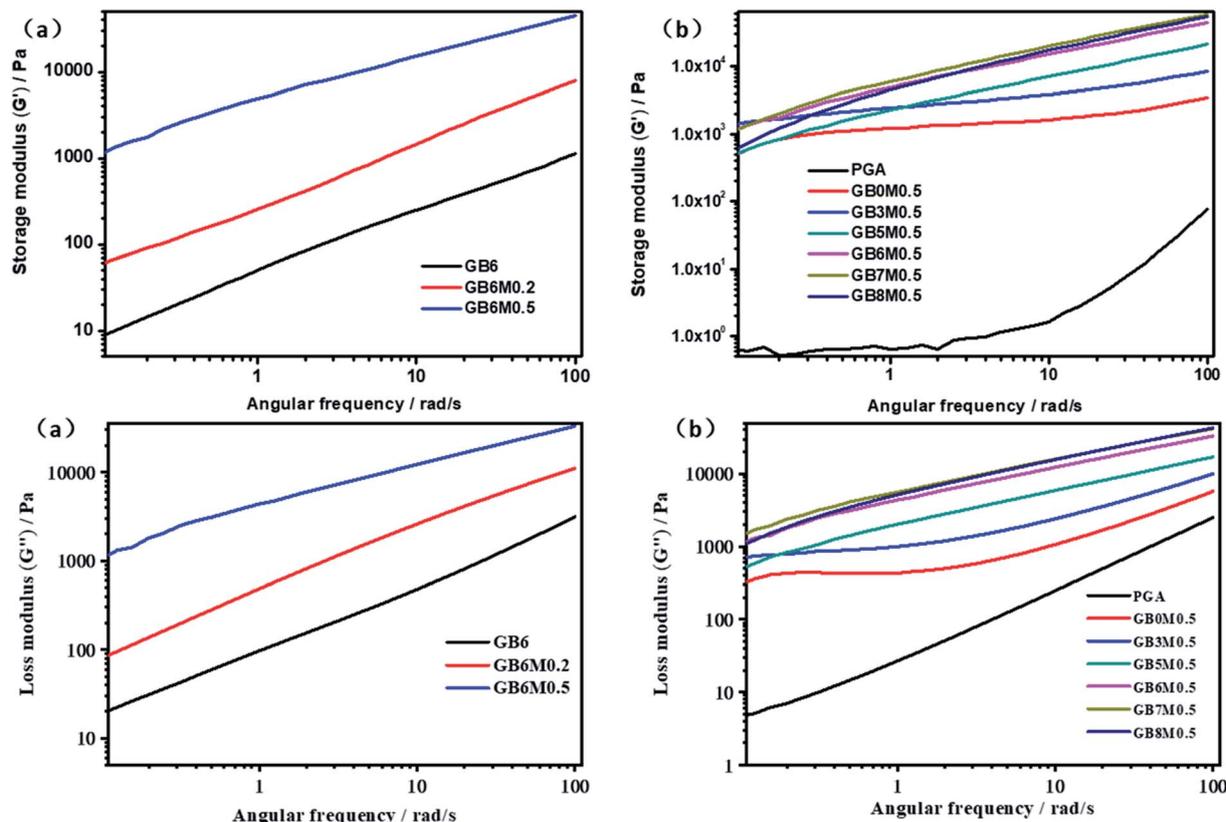**Fig. 2** Frequency dependence of storage modulus (G') and loss modulus (G''): (a): PGA/PBAT (40/60) blends with different content of MDI; (b): PGA/PBAT blends with different contents of PBAT.

PBAT achieved 80%. Due to the outstanding mechanical properties of PGA, the strength and toughness of the compatible PGA/PBAT blends could be adjusted in wide range (flexural modulus: 6.66–0.24 GPa, tensile strength: 97.3–28.4 MPa) (Table S1†). The flexural modulus and tensile strength of PGA/PBAT blends with low content of PBAT (≤30%) achieved 3.40 GPa and 58.3 MPa respectively, which were much higher than that of PLA/PBAT blends.[15]

3.4 Morphologies

The compatibility of the two phases affected greatly the performance of the system. In order to investigate the morphologies of PGA/PBAT blend, the cryo-fractured surface of impact test specimens was observed by SEM, and the results were shown in Fig. 6. When the content of PBAT was less than 70%, the system without the compatibilizer exhibited a clear
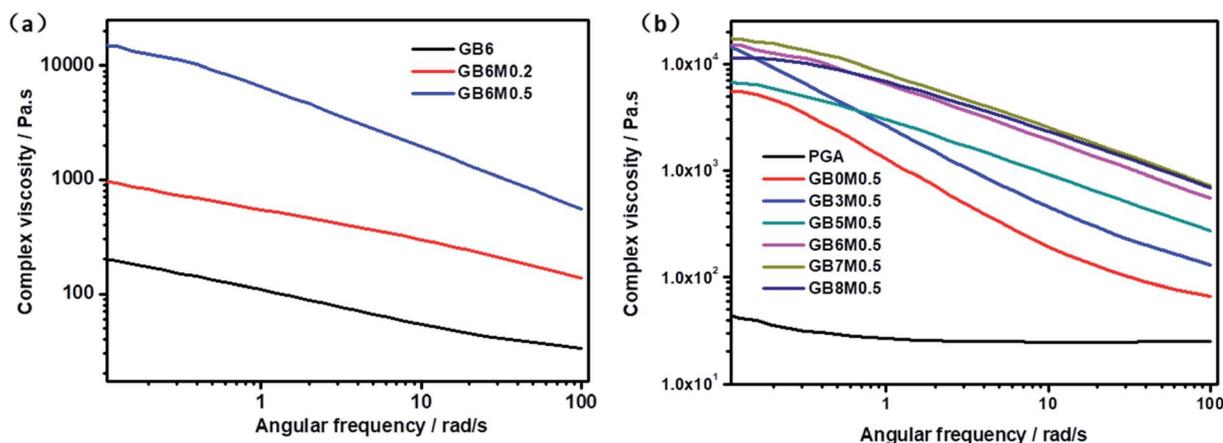

Fig. 3 Frequency dependence of complex viscosity η^*: (a): PGA/PBAT (40/60) blends with different content of MDI; (b): PGA/PBAT blends with different contents of PBAT.
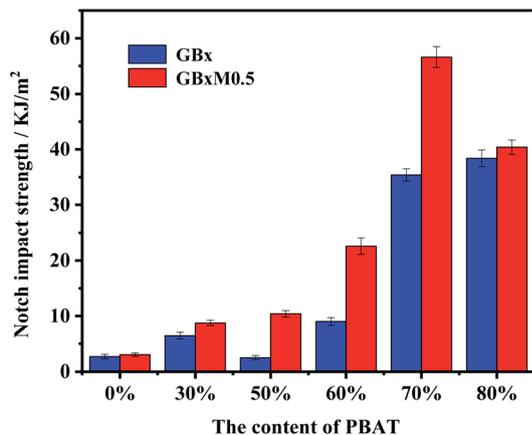
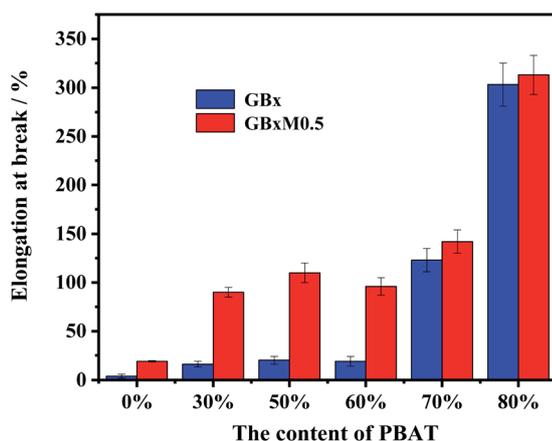Fig. 4   The impact strength of different systems.

Fig. 5   The elongation at break of different systems.

phase-separated structure. With adding MDI, the compatibility was improved. At low content of PBAT (30%), the size of dispersed phase was obviously decreased. When the PBAT content reached 50%, a small amount of microfiber was observed, and the phase-separated structure was still existed simultaneously. When the content of PBAT was increased to 60%, a uniform microfibrous phase structure was formed, and there was no obvious phase separation structure. When the PBAT content reached 80%, the system without MDI also formed a microfibrillar phase structure. In order to confirm the components of microfiber, the samples were etched with dichloromethane at room temperature to remove the PBAT, and the morphologies were listed in Fig. 6(b). The microfibers were disappeared and uniform voids were formed, which indicated that the microfibers were generated by PBAT and uniformly distributed in the PGA. This phenomenon was similar to the concept of in situ microfibrillar-reinforced composites (iMFCs), the microfibrillar structure of the reinforcing polymer within the polymer matrix was formed during processing.[33,34] But for traditional iMFCs, extra stretching was necessary, and the

component with higher melting temperatures (T_m) usually formed microfiber.[35–37] For our system, the formation of in situ microfibrillar structure just during injection molding and the microfiber formed in PBAT with relative low T_m is unexpected. We inferred that this is due to the obvious difference in mechanical strength between PGA and PBAT. During the injection molding, the PGA was easily crystallized for the high cold crystallization temperature, but due to its super high mechanical strength, it couldn't be drawn under the stress during the injection molding. On the contrary, the PBAT was in the melt state and much easier to be stretched. For the blends with low contents of PBAT (≤50%), the PGA and PBAT were incompatible and exhibited separated phase with large phases sizes. Thus the microfiber couldn't be formed. With increasing the content of PBAT (≥60%), the MDI afforded sufficient compatibility, the two components were uniformly dispersed. The strong interfacial bonding between PGA and PBAT promoted that the stress could be readily transferred from the matrix to the fibers. With high content (80%) of PBAT, the compatibility was good enough to form microfibers even without MDI. This result was in accordance with that of mechanical properties, the microfibrillar structure enhanced the interfacial bonding between the two components, which was benefit for toughness enhancement. Thus the impact strength increased sharply when this targeted structure was formed.

3.5   Thermal analysis

DSC curves and data were listed in Fig. 7 and Table 1. The temperature of cold crystallization (T_c) moved towards lower temperature accompanied by reacting with MDI, suggesting that more nucleation centers were presented in the compatible systems. We deduced that the long chain branched (LCB) structure was introduced in the blends, and the LCB polymers displayed enhanced nucleation.[38,39] But due to the chain extension reaction, which led to the increase of molecular weight, resulted in the declining mobility of the entangled chain, and inhibited the crystal growth process. Therefore, the crystallinity, enthalpy of crystallization and melting temperature were decreased. The PGA/PBAT blends show two melt endotherm peaks, suggesting that the crystals were not perfect due to the complexity of the macromolecular structure.

Due to the thermal instability of ester and high melting temperature, PGA usually decomposed during processing. Thus, the improvement of thermal stability of PGA was also important. The TGA curves (Fig. S2†) of the blends were measured under air, and the 5% decomposition temperatures were listed in Table 1. The thermal stability of pure PGA could be improved by chain extension. However, for all PGA/PBAT blends with or without MDI, the 5% decomposition temperatures were almost same. Meanwhile, the 5% decomposition temperatures of all the blending systems were increased at least in a degree of 35 °C compared to pure PGA. This result indicated that the thermal stability of PGA could be improved by blending with PBAT.
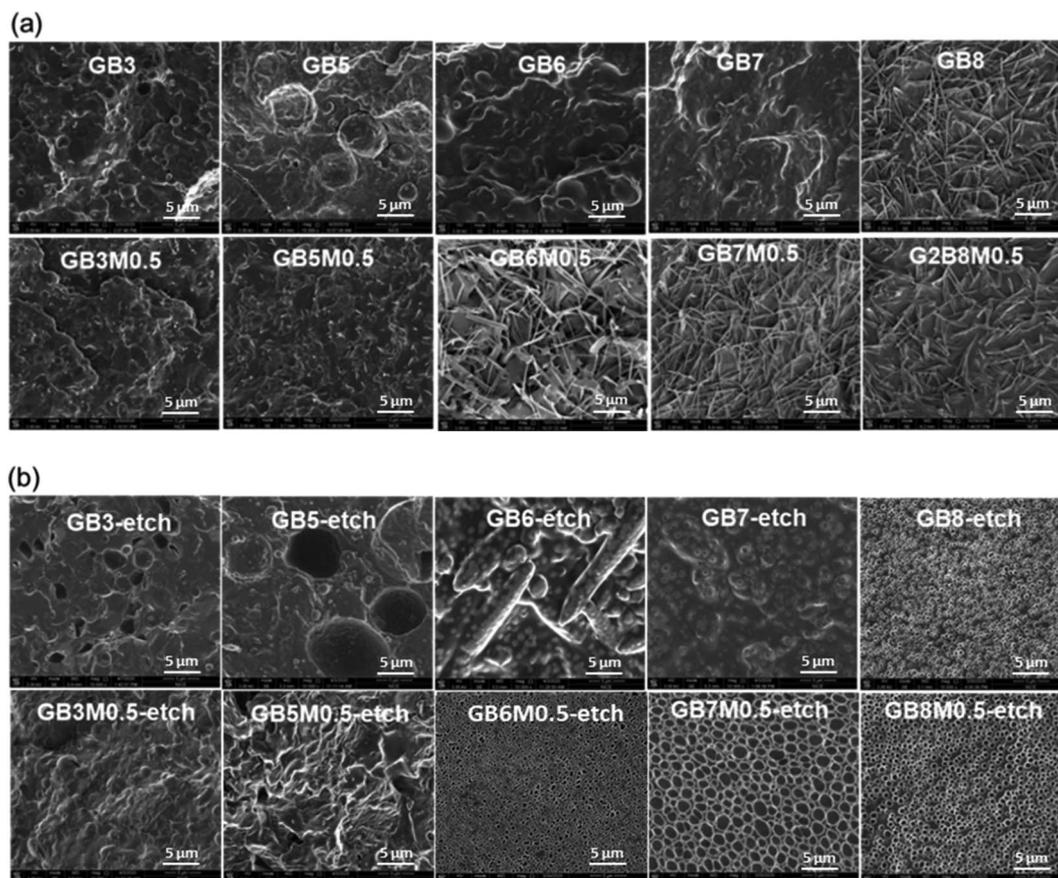
Fig. 6   SEM images of PGA/PBAT blends (a) before etch; (b) after etch.
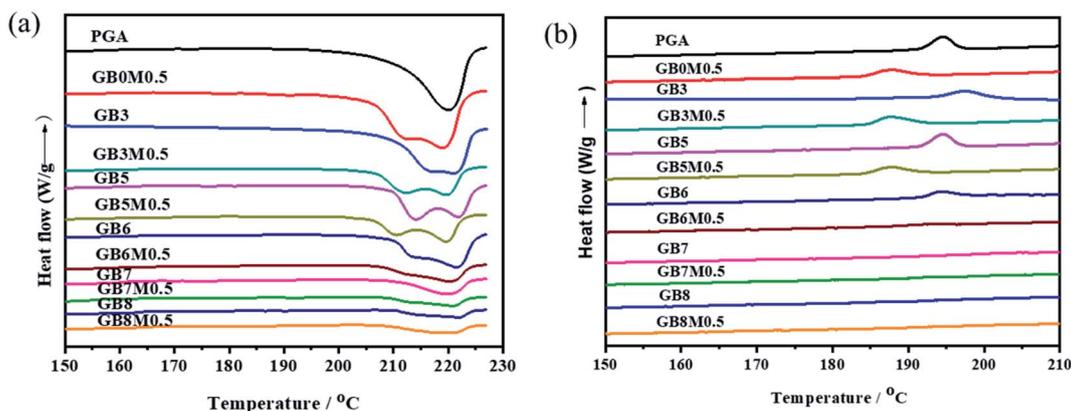

Fig. 7   DSC curves of the blends (a): second heating scans; (b) cooling scans.

3.6   POM

A polarizing microscope was used to characterize the crystallization behaviors of different samples. As can be seen from Fig. 8, PGA could form spherulites with small grain size. When MDI was added, the branched structure promoted nucleation, and more nucleation centers were formed, resulting in the decrease of grain sizes.[39] This corroborated the fact that T_c decreased as shown in DSC results. By blending PGA with PBAT,

the crystal sizes became larger. For systems without compatibilizers, the crystals were non-uniform, which was mainly due to the existence of phase separation in the system. After adding the compatibilizer, the compatibility was increased and the crystals were much more uniform, and the grain sizes were significantly reduced. This can be also explained by the fact that the notch impact of the system became significantly larger after the compatibilizer was added.

View Article Online

Paper

RSC Advances

Table 1 Thermal property of PGA/PBAT blends

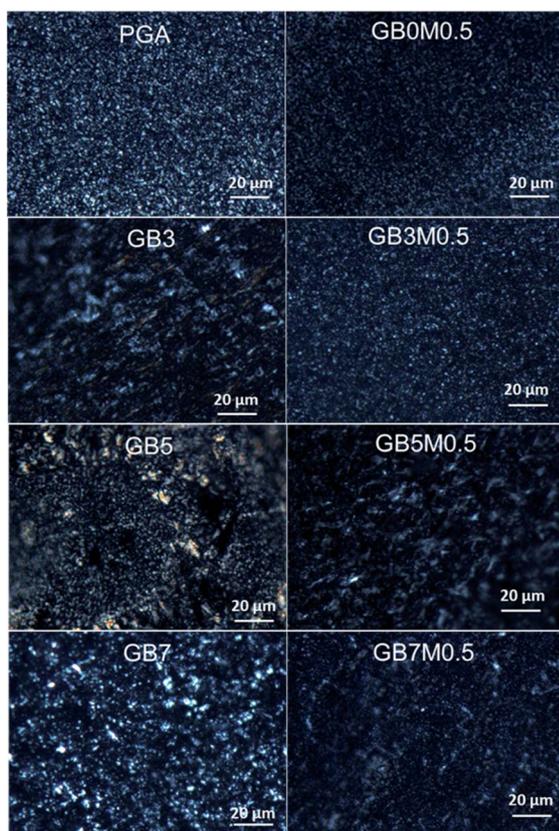| Sample	$\Delta H_{m\ PGA}/(J\ g^{-1})$	$X_{c\ PGA}$ (%)	$T_{c\ (PGA)}/^{\circ}C$	$\Delta H_{c\ PGA}/(J\ g^{-1})$	$T_m/^{\circ}C$	$T_{d5\%}/^{\circ}C$
PGA	67.6	36.9	196.1	63.6	222.0	307.0
GB0M0.5	58.6	31.9	188.3	50.3	211.6/219.0	338.5
GB3	62.1	33.9	197.4	57.0	216.8/221.0	360.5
GB3M0.5	40.6	22.2	187.5	26.4	211.7/219.5	348.0
GB5	30.2	16.5	194.5	12.7	214.2/222.3	345.2
GB5M0.5	26.8	14.6	187.9	12.3	210.2/219.2	344.0
GB6	27.8	15.2	194.3	17.8	213.5/221.6	351.6
GB6M0.5	18.9	10.3	191.8	6.4	212.3/220.1	353.0
GB7	17.1	9.3			220.3	345.2
GB7M0.5	11.0	6.0			220.7	346.5
GB8					221.9	344.8
GB8M0.5					220.4	350.2

Fig. 8 POM images of different blends.

4. Conclusion

In this work, a series of biodegradable PGA/PBAT blends with different contents of PBAT and MDI were prepared through melt processing. Due to the chain extension reaction, the complex viscosity of the blends was obviously increased by adding MDI. SEM results indicated that the compatibility of the blends was improved by *in situ* compatibilization. When the contents of PBAT lower than 60%, the dispersed phase sizes were reduced. Consequently, the impact strength and elongation at break were enhanced through reacting with MDI. But the impact strength was steady with the increase of contents of PBAT in the initial stage. However, with further increase of the contents of PBAT to 60% and 70%, an *in situ* microfibrillar structures were formed during the injection molding with the compatibilization of MDI. The interfacial adhesion was obviously increased and the impact strength of the blend was sharply improved from 9.0 kJ m^{-2} to 22.2 kJ m^{-2}. When the contents of PBAT reached 80%, the microfibrous continuous phase structures were formed even without MDI, and the mechanical properties were also not affected by MDI. The crystallinity and spherulite sizes were decreased by *in situ* compatibilization, which were benefit for enhancing the toughness of the blends. The thermal stability of the PGA was improved by blending with PBAT. The 5% thermal decomposition temperatures of all of the blends increased at least in a degree of 35 °C compared to pure PGA. Compared to PLA, due to the ultra-high strength of PGA, a series of PGA/PBAT blends with different strength and toughness can be obtained, and which can be used as a promising biopolymer to enrich the supplies of biodegradable materials.

Conflicts of interest

The authors declare no competing financial interest.

Acknowledgements

Reference

1 R. A. Gross and B. Kalra, Biodegradable polymers for the environment, *Science*, 2002, **297**, 803–807.
2 K. Van De Velde and P. Kiekens, Biopolymers: overview of several properties and consequences on their applications, *Polym. Test.*, 2002, **21**, 433–442.
3 K. Yamane and Y. Kawakami, Glycolide production process, and glycolic acid oligomer for glycolide production,

Invention patent WO02/083661 (24 October 2002), assigned to KUREHA, Corp, 2002.

4 K. Yamane and Y. Kawakami, Polyhydroxycarboxylic acid and its production process, Invention patent WO03/006525 (23 January 2003), assigned to KUREHA Corp, 2003.

5 C. Nakafuku and H. Yoshimura, Polymer, 2004, 45, 3583–3585.

6 K. Yamane, H. Miura, T. Ono, J. Nakajima and D. Ito, Crystalline polyglycolic acid, polyglycolic acid composition and production process thereof, Invention patent WO03/037956 (8 May 2003), assigned to KUREHA Corp, 2003.

7 K. Yamane, H. Sato, Y. Ichikawa, K. Sunagawa and Y. Shigaki, Development of an industrial production technology for high-molecular-weight polyglycolic acid, Polym. J., 2014, 46, 769–775.

8 M. Makaremi, H. Yousefi, G. Cavallaro, G. Lazzara, C. B. S. Goh, S. M. Lee, A. Solouk and P. Pasbakhsh, Safely dissolvable and healable active packaging films based on alginate and pectin, Polymers, 2019, 11, 1594–1611.

9 M. O. Farea, A. M. Abdelghanycd and A. H. Orabyb, Optical and dielectric characteristics of polyethylene oxide/sodium alginate-modified gold nanocomposites, RSC Adv., 2020, 10, 37621–37630.

10 G. Cavallaro, G. Lazzara and S. Milioto, Sustainable nanocomposites based on halloysite nanotubes and pectin/polyethylene glycol blend, Polym. Degrad. Stab., 2013, 98, 2529–2536.

11 G. Flodberg, I. Helland, L. Thomsson and S. BodilFredriksen, Barrier properties of polypropylene carbonate and poly(lactic acid) cast films, Eur. Polym. J., 2015, 63, 217–226.

12 D. D. Ju, L. J. Han, F. Li, S. Chen and L. S. Dong, Crystallization, mechanical properties, and enzymatic degradation of biodegradable poly(ε-caprolactone) composites with poly(lactic acid) fibers, Polym. Compos., 2013, 34, 1745–1752.

13 Y. H. Wang, K. L. Chen, C. H. Xu and Y. K. Chen, Supertoughened Biobased Poly(lactic acid)–Epoxidized Natural Rubber Thermoplastic Vulcanizates: Fabrication, Co-continuous Phase Structure, Interfacial in situ Compatibilization, and Toughening Mechanism, J. Phys. Chem. B, 2015, 119, 12138–12146.

14 S. Krishnan, P. Pandey, S. Mohanty and S. K. Nayak, Toughening of polylactic acid: an overview of research progress, Polym.-Plast. Technol. Eng., 2016, 55, 1623–1652.

15 X. P. Zhao, H. Hu, X. Wang, X. L. Yu, W. Y. Zhou and S. X. Peng, Super tough poly(lactic acid) blends: a comprehensive review, RSC Adv., 2020, 10, 13316–13368.

16 J. B. Zeng, K. A. Li and A. K. Du, Compatibilization strategies in poly(lactic acid)-based blends, RSC Adv., 2015, 5, 32546–32565.

17 G.-C. Liu, Y.-S. He, J.-B. Zeng, Y. Xu and Y.-Z. Wang, In situ formed crosslinked polyurethane toughened polylactide, Polym. Chem., 2014, 5, 2530–2539.

18 J. S. Qiu, C. Y. Xing, X. J. Cao, H. T. Wang, L. Wang, L. P. Zhao and Y. J. Li, Miscibility and Double Glass Transition Temperature Depression of Poly(L-lactic acid) (PLLA)/

Poly(oxymethylene) (POM) Blends, Macromolecules, 2013, 46, 5806–5814.

19 R. Bhardwaj and A. K. Mohanty, Modification of brittle polylactide by novel hyperbranched polymer-based nanostructures, Biomacromolecules, 2007, 8, 2476–2484.

20 S.-Y. Zhou, H.-D. Huang, X. Ji, D.-X. Yan, G.-J. Zhong, B. S. Hsiao and Z.-M. Li, Super-Robust Polylactide Barrier Films by Building Densely Oriented amellae Incorporated with Ductile in situ Nanofibrils of Poly(butylene adipate-co-terephthalate), ACS Appl. Mater. Interfaces, 2016, 8, 8096–8109.

21 D. Y. Kim, J. B. Lee, D. Y. Lee and K. H. Seo, Plasticization Effect of Poly(Lactic Acid) in the Poly(Butylene Adipate-co-Terephthalate) Blown Film for Tear Resistance Improvement, Polymers, 2020, 12, 1904–1916.

22 E. J. Dil and B. D. Favis, Localization of micro-and nano-silica particles in heterophase poly(lactic acid)/poly(butylene adipate-co-terephthalate) blends, Polymer, 2015, 76, 295–306.

23 H. Moustafa, N. E. Kissi, A. I. Abou-Kandil, M. S. Abdel-Aziz and A. Dufresne, PLA/PBAT bionanocomposites with antimicrobial natural rosin for green packaging, ACS Appl. Mater. Interfaces, 2017, 9, 20132–20141.

24 Z. Q. Sun, B. Zhang, X. C. Bian, L. D. Feng, H. Zhang, R. L. Duan, J. R. Sun, X. Pang, W. Q. vChen and X. S. Chen, Synergistic effect of PLA–PBAT–PLA tri-block copolymers with two molecular weights as compatibilizers on mechanical and rheological properties of PLA/PBAT blends, RSC Adv., 2015, 5, 73842–73849.

25 S. Girdthep, N. Komrapit, R. Molloy, S. Lumyong, W. Punyodom and P. Worajittiphon, Effect of plate-like particles on properties of poly(lactic acid)/poly(butylene adipate-co-terephthalate) blend: a comparative study between modified montmorillonite, P. Compos. Sci. Technol., 2015, 119, 115–123.

26 L. Jiang, M. P. Wolcott and J. Zhang, Study of Biodegradable Polylactide/Poly(butylene adipate-co-terephthalate) Blends, Biomacromolecules, 2006, 7, 199–207.

27 P. Ma, X. Cai, Y. Zhang, S. Wang, W. Dong, M. Chen and P. J. Lemstra, In situ compatibilization of poly(lactic acid) and poly(butylene adipate-co-terephthalate) blends by using dicumyl peroxide as a free-radical initiator, Polym. Degrad. Stab., 2014, 102, 145–151.

28 N. W. Zhang, Q. F. Wang, J. Ren and L. Wang, Preparation and properties of biodegradable poly(lactic acid)/poly(butylene adipate-co-terephthalate) blend with glycidyl methacrylate as reactive processing agent, J. Mater. Sci., 2009, 44, 250–256.

29 B. H. Li and M. C. Yang, Improvement of thermal and mechanical properties of poly(L-lactic acid) with 4,4-methylene diphenyl diisocyanate, Polym. Adv. Technol., 2006, 17, 439–443.

30 F. Zhao, H. X. Huang and S. D. Zhang, Largely toughening biodegradable poly(lactic acid)/thermoplastic polyurethane blends by adding MDI, J. Appl. Polym. Sci., 2015, 132, 42511–42519.

31 H. Wang, X. Sun and P. J. Seib, Mechanical properties of poly(lactic acid) and wheat starch blends with methylenediphenyl diisocyanate, *J. Appl. Polym. Sci.*, 2002, **84**, 1257–1262.

32 H. W. Pan, Z. L. Li, J. Yang, X. Li, X. Ai, Y. P. Hao, H. L. Zhang and L. S. Dong, The effect of MDI on the structure and mechanical properties of poly(lactic acid) and poly(butylene adipate-*co*-butylene terephthalate) blends, *RSC Adv.*, 2018, **8**, 4610–4623.

33 M. Evstatiev, S. Fakirov, G. Bechtold and K. Friedrich, Structure–property relationships of injection-and compression-molded microfibrillar-reinforced PET/PA-6 composites, *Adv. Polym. Technol.*, 2000, **19**, 249–259.

34 Z. M. Li, M. B. Yang, R. Huang, W. Yang and J. M. Feng, Poly(ethylene terephthalate)/polyethylene composite based on *in situ* microfiber formation, *Polym.-Plast. Technol. Eng.*, 2002, **41**, 19–32.

35 X. J. Sun, Q. Yu, J. B. Shen, S. l. Gao, J. Li and S. Y. Guo, *In situ* microfibrillar morphology and properties of polypropylene/ polyamide/carbon black composites prepared through multistage stretching extrusion, *J. Mater. Sci.*, 2013, **48**, 1214–1224.

36 J. B. Shen, M. Wang, J. Li and S. Y. Guo, *In situ* fibrillation of polyamide 6 in isotactic polypropylene occurring in the laminating-multiplying die, *Polym. Adv. Technol.*, 2011, **22**, 237–245.

37 M. Evstatiev and S. Fakirov, Microfibrillar reinforcement of polymer blends, *Polymer*, 1992, **33**, 877–880.

38 L. Wang, D. Wan, Z. J. Zhang, F. Liu, H. P. Xing, Y. H. Wang and T. Tang, Synthesis and Structure-Property Relationships of Polypropylene-*g*-poly(ethylene-*co*-1-butene) Graft Copolymers with Well-Defined Long Chain Branched Molecular Structures, *Macromolecules*, 2011, **44**, 4167–4179.

39 V. Ojijo and S. S. Ray, Super toughened biodegradable polylactide blends with non-linear copolymer interfacial architecture obtained *via* facile *in situ* reactive compatibilization, *Polymer*, 2015, **80**, 1–17.